

REMARKS

Claims 1-26 are pending. Claims 1, 10, 13, and 24 are in independent form.

As a threshold matter, Applicant notes that substitute Form PTO-1449's appended to with the Office action mailed June 13, 2007 do not appear to be associated with this application. Instead, these substitute Form PTO-1449's appear to be associated with U.S. Patent Application No. 11/101,653. Applicant respectfully requests that the status of these substitute Form PTO-1449's, and the references cited therein, be clarified.

Further, enclosed herewith is a copy of the Information Disclosure Statement filed in the present application on March 15, 2004, along with a date-stamped postcard identifying receipt of the Information Disclosure Statement by the OIPE. Applicant respectfully requests that the reference cited therein be considered in the present application.

In the action mailed June 13, 2007, claims 18, 19-21, and 6 were objected to on various grounds. These claims have been amended to address the Examiner's concerns.

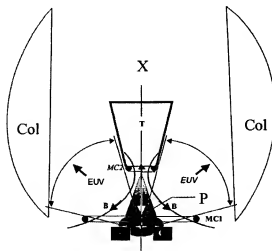
Rejections under 35 U.S.C. § 102(e)

Claim 1 was rejected under 35 U.S.C. § 102(e) as anticipated by U.S. Patent Publication No. 2005/0140945 to Banine et al. (hereinafter "Banine").

Claim 1 relates to a apparatus that includes a plasma produced light source, one or more collector optics, and a magnetic field generator operative to generate a magnetic field around the one or more collector optics. The magnetic field generator comprises windings around a non-reflective surface in the one or more collector optics.

The rejection of claim 1 contends that Banine's magnetic coils MC1, MC2 are magnetic field generator operative to generate a magnetic field around the one or more collector optics, as recited in claim 1.

Applicant respectfully disagrees. For the sake of convenience, FIG. 6 of Banine is now reproduced.



As shown, magnetic coils MC1, MC2 do not generate magnetic field B around collector Col. Indeed, Banine describes that this arrangement of causes the plasma containing debris particles to tend to move towards the electrodes, rather than spreading out towards the collector Col. See Banine, para. [0072].

It is well-established that anticipation requires that a reference shows the recited subject matter "in as complete detail as is contained in the ... claim." See, e.g., *M.P.E.P.* §2131 (citing *Richardson v. Suzuki Motor Co.*, 868 F.2d 1226, 1236, (Fed. Cir. 1989)). In the present case, Banine fails to describe or suggest a magnetic field generator that is operative to generate a magnetic field around one or more collector optics, as recited in claim 1.

Accordingly, claim 1 is not anticipated by Banine. Applicant respectfully requests that the rejections of claim 1 and the claims dependent therefrom be withdrawn.

Claim 10 was rejected under 35 U.S.C. § 102(e) as anticipated by Banine.

Claim 10 relates to an apparatus that includes a plasma produced light source, one or more collector optics, and a magnetic field generator operative to generate a magnetic field around the one or more collector optics. The magnetic field

generator comprises a solenoid structure adjacent a non-reflective surface in the one or more collector optics.

As discussed above, Banine's magnetic coils MC1, MC2 do not generate magnetic field B around collector Col. Thus, Banine fails to describe or suggest a magnetic field generator that is operative to generate a magnetic field around one or more collector optics.

Accordingly, claim 10 is not anticipated by Banine. Applicant respectfully requests that the rejections of claim 10 and the claims dependent therefrom be withdrawn.

Claim 13 was rejected under 35 U.S.C. § 102(e) as anticipated by Banine.

Claim 13 relates to a method that includes generating a magnetic field around collector optics in a lithography system with windings around a non-reflective surface in the collector optics and deflecting debris particles generated by a plasma producing light source from a reflective surface in the collector optics.

As discussed above, Banine's magnetic coils MC1, MC2 do not generate magnetic field B around collector Col. Thus, Banine fails to describe or suggest generating a magnetic field around collector optics with windings around a non-reflective surface in the collector optics, as recited in claim 13.

Accordingly, claim 13 is not anticipated by Banine.

Applicant respectfully requests that the rejections of claim 13 and the claims dependent therefrom be withdrawn.

Claim 24 was rejected under 35 U.S.C. § 102(e) as anticipated by Banine.

Claim 24 relates to a method that includes generating a magnetic field around collector optics in a lithography system with a solenoid structure adjacent a non-reflective surface in the collector optics and deflecting debris particles generated by a plasma producing light source from a reflective surface in the collector optics.

As discussed above, Banine's magnetic coils MC1, MC2 do not generate magnetic field B around collector Col. Thus, Banine fails to describe or suggest generating a magnetic field around collector optics with a solenoid structure, as recited in claim 24.

Accordingly, claim 24 is not anticipated by Banine. Applicant respectfully requests that the rejections of claim 24 and the claims dependent therefrom be withdrawn.

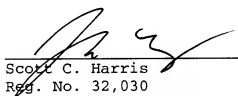
It is believed that all of the pending claims have been addressed. However, the absence of a reply to a specific rejection, issue, or comment does not signify agreement with or concession of that rejection, issue, or comment. In addition, because the arguments made above may not be exhaustive, there

may be reasons for patentability of any or all pending claims (or other claims) that have not been expressed. Finally, nothing in this paper should be construed as an intent to concede any issue with regard to any claim, except as specifically stated in this paper, and the amendment of any claim does not necessarily signify concession of unpatentability of the claim prior to its amendment.

Applicant asks that all claims be allowed. No fees are believed due at this time. Please apply any credits or additional charges to deposit account 06-1050.

Respectfully submitted,

Date: September 7, 2007



Scott C. Harris
Reg. No. 32,030

Fish & Richardson P.C.
PTO Customer No. 20985
12390 El Camino Real
San Diego, California 92130
(858) 678-5070 telephone
(858) 678-5099 facsimile


BY
JOHN F. CONROY
REG. NO. 45,485

SCH/JFC/jhg
10763532.doc

RECEIVED

MAR 22 2004

FISH & RICHARDSON, P.C.
SAN DIEGO

Attorney's Docket No. 10559-888001	Express Mail Label No.	Mailing Date March 15, 2004	<i>For PTO Use Only</i> <i>Do Not Mark in This Area</i> 
Application No. 10/759,344	Filing Date January 15, 2004	Attorney/Secretary Init KSJ/smr	
Title of the Invention EROSION MITIGATION FOR COLLECTOR OPTICS USING ELECTRIC AND MAGNETIC FIELDS			
Applicant Lee et al.			
Client Reference No. P17739			
Inclosures ·Information Disclosure Statement (2 pages) ·Form PTO-1449 (1 page) ·Documents listed on the Form PTO-1449 (2 documents listed & enclosed)			

IN THE UNITED STATES PATENT AND TRADEMARK OFFICE

Applicant : Lee et al. Art Unit: to be assigned
Serial No.: 10/759,344 Examiner: to be assigned
Filed : January 15, 2004 Assignee: Intel Corporation
Title : EROSION MITIGATION FOR COLLECTOR OPTICS USING
ELECTRIC AND MAGNETIC FIELDS

Commissioner for Patents
P.O. Box 1450
Alexandria, VA 22313-1450

INFORMATION DISCLOSURE STATEMENT

Dear Sir:

Applicants call attention to the attached Information
Disclosure Statement and documents listed on form PTO-1449.

This filing is being made before the receipt of a first
Office action on the merits. No fee is required.


The documents are in the English language; hence no concise
explanation is necessary per Rule 98(a)(3).

Consideration of the foregoing and enclosures plus the
return of a copy of the enclosed form PTO-1449 with the
Examiner's initials in the left column per MPEP 609 are
earnestly solicited along with an early action on the merits.

CERTIFICATE OF MAILING BY FIRST CLASS MAIL

I hereby certify under 37 CFR §1.8(a) that this correspondence is being
deposited with the United States Postal Service as first class mail with
sufficient postage on the date indicated below and is addressed to the
Commissioner for Patents, P.O. Box 1450, Alexandria, VA 22313-1450.

REPORTED
TO INTEL

March 15, 2004
Date of Deposit
Signature 
Norman Green
Typed or Printed Name of Person Signing Certificate

Please apply any additional charges or credits to Deposit
Account No. 06-1050.

Respectfully submitted,

Date: _____

3/15/04



Scott C. Harris

Reg. No. 32,030

Attorney for Intel Corporation

Fish & Richardson P.C.
USPTO Customer No. 20985
12390 El Camino Real
San Diego, CA 92130
Telephone: (858) 678-5070
Facsimile: (858) 678-5099

/BY
KENYON JENCKES
REG. NO. 41,873

Substitute Form PTO-1449 (Modified)	U.S. Department of Commerce Patent and Trademark Office	Attorney's Docket No. 10559-888001	Application No. 10/759,344
Information Disclosure Statement by Applicant (Use several sheets if necessary) (37 CFR §1.98(b))		Applicant Lee et al.	
		Filing Date January 15, 2004	Group Art Unit to be assigned

U.S. Patent Documents

Examiner Initial	Desig. ID	Document Number	Publication Date	Patentee	Class	Subclass	Filing Date If Appropriate
	AA						
	AB						
	AC						
	AD						

Foreign Patent Documents or Published Foreign Patent Applications

Examiner Initial	Desig. ID	Document Number	Publication Date	Country or Patent Office	Class	Subclass	Translation	
							Yes	No
	AE							
	AF							
	AG							
	AH							

Other Documents (Include Author, Title, Date, and Place of Publication)

Examiner Initial	Desig. ID	Document
	AI	Tsai <i>et al.</i> , "Different electrostatic methods for making electret filters," Jnl. of Electrostatics 54 (2002), pp. 333-341.
	AJ	Kravtsov <i>et al.</i> , "Analysis of the polarization state of melt-spun polypropylene fibers," Jnl. of Materials Proc. Technol., 124 (2002), pp. 160-165.
	AK	
	AL	

Examiner Signature	Date Considered
EXAMINER: Initials citation considered. Draw line through citation if not in conformance and not considered. Include copy of this form with next communication to applicant.	

Different electrostatic methods for making electret filters

Peter P. Tsai^{a,*}, Heidi Schreuder-Gibson^b, Phillip Gibson^b

^a *Textiles and Nonwovens Development Center (TANDEC), The University of Tennessee,
1321 White Avenue, Knoxville, TN 37996-1950, USA*

^b *U.S. Army Soldier Systems Command, Natick Research, Development and Engineering Center,
Natick, MA, USA*

Received 10 August 2000; received in revised form 24 March 2001; accepted 31 March 2001

Abstract

Three charging techniques (viz., corona charging, tribocharging, and electrostatic fiber spinning) were used to charge fibers or fabrics of different polymer types. Corona charging is suitable for charging monopolymer fiber or fiber blend, or fabrics. Tribocharging is only appropriate for charging fibers with dissimilar electronegativity. Electrostatic fiber spinning combines the charging of polymer and the spinning of the fibers as a one-step process. It was observed that two dissimilar fibers following tribocharging had higher filtration efficiency than the corona-charged polypropylene fibers. An electrostatic spinning process produced nanofibers exhibiting extremely high efficiency by mechanical filtration mechanisms. Little charge was retained in electrospun polyethylene oxide fibers; however, polycarbonate and polyurethane retained a great amount of charge. © 2002 Elsevier Science B.V. All rights reserved.

Keywords: Corona charging; Tribocharging; Electrostatic spinning; Electret; Filter

1. Introduction

Fibrous materials used for filter media provide advantages of high filtration efficiency (FE) and low air resistance. Electrostatic charging of the media improves their FE by the electrostatic attraction of particles without the increase of pressure drop [1]. Three techniques (viz., electrostatic spinning (ES) [2], corona charging [3] and tribocharging [4]) are used to make and/or to charge the fibers or the fabrics. This paper compares the FE and the surface charge potential of these three

*Corresponding author. Tel.: +1-865-974-2616; fax: +1-865-974-3580.
E-mail address: ppytsai@utk.edu (P.P. Tsai).

techniques. The processes for making the media are addressed and the media properties presented.

2. Experimental design

Meltblown (MB) fabrics of basis weights 17, 25, 70 and 100 g/m², and spunbond (SB) of 35 g/m², received corona charging. Two types of needle-punched felts having basis weights ranging from 60 to 160 g/m² were supplied by Texel, Canada. One was three denier 100% polypropylene (PP) which was corona charged using TANTRET Tech-I and T-II [5]. The other one contained two dissimilar electrical properties of fibers, PP and specialty fibers, and was charged by triboelectrification during the textile carding process. Three polymer solutions (viz., polyethylene oxide (PEO), polycarbonate (PC) and polyurethane (PU)) were used to make ES fibers. PEO solution was prepared by dissolving 10% PEO in 80% isopropyl alcohol (IPA) and 10% water. PC solution was made by dissolving in dimethylformamide (DMF) and tetrahydrofuran (THF) at a ratio of 1:1 for a concentration of 20% by weight. PU was dissolved in DMF for a concentration of 10%. Fabric weight from 3–10 g/m² were electrospun for this study.

Fig. 1 presents the electrospinning process onto a stationary flat collector for this paper. The ES process consists of a pipette for the reservoir of the polymer solution as well as for the spinning nozzle, a grounded surface for collecting the fibers to make nonwoven web, and a SIMCO high-voltage DC power supply having maximum voltage of 50 kV and amperage of 2 mA to generate electrostatic charges. The



Fig. 1. An electrospinning process onto stationary flat collector, collector scale 1:6.

high-voltage electrode is directly introduced into the solution from the top end of the pipette. The distance between the bottom end of the pipette to the collector is 30 cm. Fiber production rate from a single orifice is typically in the range of 10–100 mg fiber per min.

Surface-charge potential of the fabrics was measured by the scanning system [1] developed at the University of Tennessee. Generally, the surface-charge potential of a charged media either by corona charging or by triboelectrification, before or after heat treatment, has a high coefficient of variation (CV), about 50%. Therefore, 400 scans (20×20 for *x*- and *y*-axis), 2.54 cm apart between scans, were measured. Arithmetic and absolute averages as well as the CV were computed from the 400 scanned data. Absolute average is the arithmetic average of the absolute values. It is important to correlate FE and absolute average of surface-charge potential if the media has a randomly distributed positive and negative charges because they both contribute to FE and their arithmetic average cancels them out.

An automatic filtration tester, TSI 8110, that generated NaCl aerosol having a number mean particle size of $0.1 \mu\text{m}$ and geometric standard deviation of 1.9 at a face velocity of 5.3 cm/s was used to test the media FE. Aerosol of dioctyl phthalate (DOP) at a velocity of 9.1 cm/s was also used to load the ES fabrics for charge-retention testing. DOP had a number mean particle size of $0.2 \mu\text{m}$ and a geometric standard deviation of 1.6. FE decay of the media was accelerated by heating to 60°C , 90°C and 120°C for needled felts and 110°C , 120°C and 130°C for MB fabrics using a Werner Mathis AG through-air laboratory oven. The fiber diameter of MB fabrics is around $2 \mu\text{m}$ and of needled felts is $25 \mu\text{m}$. Higher temperature treatment is needed for MB fabrics in order to observe their FE decay because they have better charge-retention ability. The CV of the media FE is around 5%. Therefore, six FE tests were measured for each sample and the average was calculated.

3. Results and discussion

Basis weight and FE of the needled felt media charged by corona and triboelectrification are summarized in Table 1. These three corona-charged felts

Table 1
Basis weight and filtration efficiency of corona-charged and triboelectrified needled felts

Sample		B. weight (g/m ²)	FE (%)	ΔP (mm H ₂ O)	FE normalized to 100 g/m ²
Corona	1	100	75.7	0.18	75.7
	2	70 (15SB + 55 felt)	64.5	0.2	77.2
	3	160	87.5	0.9	72.7
Tribo	4	130	97.8	0.55	94.7
	5	120	97.3	0.8	95.1
	6	60	83	0.4	94.8

had an average FE of 75% after being normalized to 100 g/m² while the three triboelectrified had an average FE of 95%. Please note that Sample 5 had a lower basis weight but exhibited a higher pressure drop (Δp) than Sample 4 because it was made denser for application purpose. A dense needled fabric increases its mechanical strength but not really FE as shown in the table. Triboelectrified media had 1.27 times higher FE than that of corona-charged. However, triboelectrified materials contain two dissimilar fibers of different electronegative properties, usually PP and modacrylics. Modacrylics is expensive and both fibers need to be highly cleaned in order to generate triboelectrification effect. The static charges produced by triboelectrification also increase the difficulty in the carding process. Fibers for corona-charged felts are usually PP produced from a fiber spinning process containing spin finish that eliminates charge retention on the media. However, the charge retention problem can be resolved if spin finish with little antistatic agent is carefully chosen.

Fig. 2 compares the FE decay rates of Samples 1 and 4 in Table 1 as a function of the duration of heat treatment time at temperatures of 60°C, 90°C and 120°C. The percentage of the FE decay in terms of filtration index after 60-min heat treatment, indicated on each series, showed that corona-charged fabrics had a higher decay rates than those triboelectrified (viz., 31.2% vs. 24.1%, etc.) Filtration index is defined as

$$\mu = \frac{\ln(1/p)}{\Delta p}, \quad (1)$$

where μ is the filtration index, p the penetration, Δp the pressure drop.

It is essential to use filtration index to compare the FE decay rather than the FE percentage, e.g., the decay of the FE from 99% to 90% is 9.1% in FE but 50% in filtration index. An FE of 90% is equivalent to the FE of 50% of the weight of a 99% FE media.

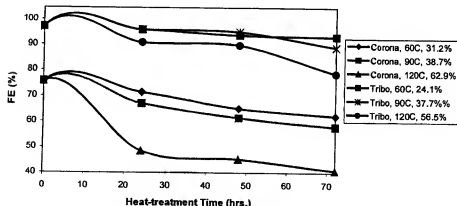


Fig. 2. FE decay rates of corona-charged and tribocharged felts as a function of the duration of heat treatment at different temperatures.

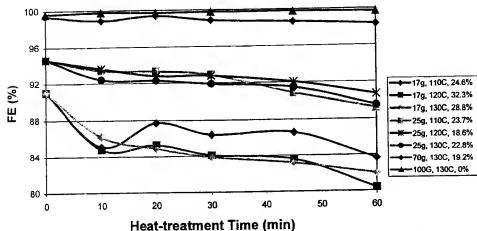


Fig. 3. FE decay rates of different weight meltblown fabrics as a function of the duration of heat treatment at different temperatures.

Table 2

Surface-charge potential measurements of corona-charged and triboelectrified felts

No. Sample	Surface-charge measurements (V)					
	Face side			Back side		
	Arith. Avg.	Absolute Avg.	CV (%)	Arith. Avg.	Absolute Avg.	CV (%)
1 Sample 1, Table 1. T-I	304	357	89	-221	274	115
2 Sample 1, Table 1. T-II	1035	1121	52	-984	1012	58
3 Sample 4, Table 1	974	1000	43	-556	556	50
4 #3 recharged by T-II	1429	1442	36	-1386	1386	23
5 #3 normalized to 100 g/m ²	749	769	—	-428	428	—
6 #4 normalized to 100 g/m ²	1099	1109	—	-1066	1066	—

Fig. 3 shows the FE decay rates of corona-charged MB fabrics for four basis weights (viz., 17, 25, 70 and 100 g/m²) as a function of the duration of heat treatment at three temperatures (viz., 110°C, 120°C and 130°C). These had much lower decay rates than those of corona-charged needled felts as indicated by the reduction of filtration index shown on each series in the chart. Higher basis weight of MB fabrics had a lower decay rate than lower basis weight. Furthermore, needled felts were much more porous than MB fabrics so their decay rate behaves like the MB fabrics of lower basis weight, which have higher decay rate.

Table 2 lists the surface-charge potential measurements on both sides of the media of Samples 1 and 4 in Table 1. After normalizing to 100 g/m², triboelectrified felts had a higher surface-charge potential than that of corona-charged by T-I but lower potential than corona-charged by T-II. When the charges on the triboelectrified felts

were neutralized by washing using IPA and corona-recharged using Tech-II, they showed higher surface-charge potential but lower FE than the original triboelectrified felts. Tech-II charged media to a higher surface-charge potential but lower FE for lower basis weight media as observed by our previous research [1]. Both corona-charged and triboelectrified felts had a similar amount of surface-charge potential but opposite polarities on both sides of the media. This means that they both behave like bipolar materials. This is a typical result of charged materials and this property is believed to increase the FE of neutral aerosols because the bipolar electric field polarizes the neutral aerosols, and to increase the media charge-retention ability because the positive and negative charges attract each other. Fig. 4 illustrates the FE of triboelectrified felt of Sample 4 in Table 1 before and after IPA washing, and corona-recharged after washing. Felts made of dissimilar fibers can be well triboelectrified. Therefore, their FE were greatly improved. When these felts were corona-charged, the FE was lower than the original triboelectrified media.

Fig. 5 presents SEM photomicrographs of ES fibers made from PC, PU and PEO, showing similar and uniform fiber diameter in the range of 0.1–0.5 μm . Fig. 6 shows the penetration, a value of FE subtracted from 100%, of these three media by loading with DOP. Please note that penetration curve is commonly preferred to describe the FE decay with the particle loading. Both PC and PU had a higher initial FE, then decreased after DOP loading because they retained the charge from ES and the charge was neutralized by DOP. In contrast, PEO did not have the FE decay characteristic because it did not retain the charge. This why it did not have higher initial FE.

PEO had a lower basis weight (3 g/m^2) than PC and PU. Therefore, its FE was lower as was its pressure drop (Fig. 7). PU had a sharp increase in pressure drop by DOP loading because the fibers were swelled by DOP adsorption. The swollen fibers occupied the pores between the fibers.

The FE of PEO web is purely mechanical. However, the NaCl FE (78%) of the 3 g/m^2 PEO is equivalent to that of 100 g/m^2 of uncharged MB and to 1000 g/m^2 of uncharged spunbond (SB) fabric. Table 3 compares the FE of uncharged SB and MB

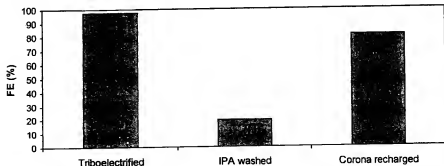


Fig. 4. Filtration efficiency of triboelectrified needed felt, charge neutralized by IPA and then corona-recharged.

PC



PU



PEO



Fig. 5. SEM photomicrographs of three ES fiber samples.

fabrics, charged felts and electrospun PEO web at different basis weights and normalized to 10 g/m^2 . It is interesting to note that a basis weight of 16.1 g/m^2 PEO electrospun web can achieve the FE of a HEPA (high efficiency particulate air) filter, i.e. 99.97%.

Fibers having different diameters ranging from nanometers to micrometers can be produced from numerous polymers by the electrospinning process [6,7]. The charge-

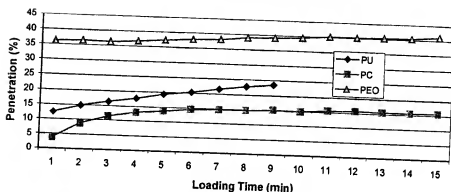


Fig. 6. Penetration of three ES samples with DOP loading as a function of time.

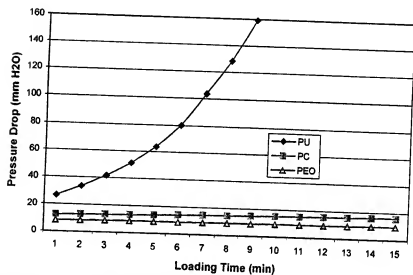


Fig. 7. Pressure drop of the three ES samples in Fig. 6 loading with DOP as a function of time.

Table 3
Comparison of FE for different nonwoven-making processes

Sample	FE (%)	FE (%) normalized to 10 g/m ²
SB (35 g/m ²), corona-charged, T-I	37.2	9.5
MB (35 g/m ²), corona-charged, T-I	98.6	70.5
Triboelectrified felt (130 g/m ²)	97.8	25.4
Corona-charged felt (100 g/m ²), T-II	75.7	13.2
Electrospun PEO (3 g/m ²), uncharged	78	99.4

retention ability by this process as well as by other electrostatic charging processes such as corona charging and triboelectrification depends on the electrical properties such as conductivity and dielectric constant of the polymers rather than on the charging techniques [8]. Fibers produced from ES polycarbonate have good charge retention and have been commercially used for vehicle cabin-air filters [9].

4. Conclusions

Corona charging, triboelectrification and electrostatic spinning are three techniques for making charged media for filters. FE depends on the charging techniques while charge retention is independent of but depends on the electrical properties of the polymers as well as the fiber diameter and the media structure. Charged media produced by triboelectrification has a higher charge density and FE but charging can only be achieved in the carding process and it requires two dissimilar electronegative properties of the fibers. Both corona charging and triboelectrification are able to produce bipolar materials. Corona charging can also greatly improve the FE on the uncharged materials for triboelectrification but not so significant as by triboelectrification. Corona charging is applicable to both fibers and fabrics but it is superior to charge higher density fabrics than lower density ones. Fibers are charged in electrospinning process and this process can produce very fine fibers but the production speed per spinning nozzle is slow.

References

- [1] P.P. Tsai, L.C. Wadsworth, Electrostatic charging of meltblown webs for high-efficiency air filters, in: *Advances in Filtration and Separation Technology*, American Filtration and Separation Society, Vol. 9, 1995, pp. 473–491.
- [2] J. Doshi, D.H. Reneker, Electrospinning process and applications of electrospun fibers, *J. Electrostat.* 35 (1995) 151–160.
- [3] P.P. Tsai, L.C. Wadsworth, Theory and techniques of electrostatic charging of meltblown nonwoven webs, *TAPPI J.* 81 (1) (1998) 274–278.
- [4] P.A. Smith, G.C. East, R.C. Brown, D. Wake, Generation of triboelectric charge in textile fibre mixtures and their use as air filters, *J. Electrostat.* 21 (1988) 81–98.
- [5] P.P. Tsai, L.C. Wadsworth, US Patent 5, 406, 446.
- [6] D.H. Reneker, I. Chun, Nanometre diameter fibres of polymer, produced by electrospinning, *Nanotechnology* 7 (1996) 216–223.
- [7] L. Larronds, J. Manley, Electrostatic fiber spinning for polymer melts, I. Experimental observations on fiber formation properties, *J. Polym. Sci.: Polym. Phys. Ed.* 19 (1981) 909–920.
- [8] P.P. Tsai, L.C. Wadsworth, Effect of polymer properties on the electrostatic charging of different media structures for air filters, *Conference Proceedings, SPE, ANTEC '96*, Indianapolis, May 5–10, pp. 3642–3661.
- [9] J. Sievert, Electrostatically spun microfiber nonwovens as filter media in air filtration, *Book of Papers, INDA's Filtration Conference*, Wyndham Franklin Plaza Hotel, Philadelphia, PA, March 12–14, 1991, pp. 87–96.

Analysis of the polarization state of melt-spun polypropylene fibers

A.G. Kravtsov^{a,*}, H. Brünig^b, S.F. Zhandarov^b

^aV.A. Belyi Metal-Polymer Research Institute, National Academy of Sciences of Belarus, Kirov Str. 32a, 246652 Gomel, Belarus

^bInstitute of Polymer Research, Hohe Str. 6, 01069 Dresden, Germany

Received 12 September 2000; accepted 5 March 2002

Abstract

In this work, melt-spun polypropylene fibers were treated in an electric field of corona discharge. The fibers were then characterized using thermally stimulated current spectroscopy. It has been shown that the electret state of corona treated polypropylene fibers is a result of combination of three different effects: Maxwell–Wagner polarization, dipole polarization and charge trapping. The electret state induced in polypropylene fibers by the corona discharge treatment holds for a long time (several months). Our analysis of the effect of processing temperature and electric field intensity on the characteristics of the electret state in melt-spun polypropylene fibers allows one to specify optimal technological regimes for industrial production of polypropylene-based electret materials. © 2002 Published by Elsevier Science B.V.

Keywords: Melt-spun fibers; Thermally stimulated current; Electrization; Spontaneous polarization; Electret effect; Corona discharge

1. Introduction

During the melt-spinning process of polymer fiber formation, individual filaments are drawn at the rate of 1000–6000 m/min (usually 2000–3000 m/min), i.e., the time of action of basic technological factors is less than 0.1 s. The main relationships between polymer properties, technological parameters of the formation process and the physico-mechanical properties of the fibers have been obtained using several physical and analytical models [1–3].

The properties of melt-spun fibers are determined, to a great extent, by the temperature and mechanical stress in the fiber in the region from the spinning die to the point of solidification. Tensile stress at the point of solidification affects the degree of macromolecules orientation and correlates with the fiber elongation to break. The latter is of interest for technologists because it has considerable effect on physico-mechanical properties of the fibers.

When a spinning head with large number of holes is used in the melt-spinning process, individual fibers are differently cooled and stressed in the formation region [4]. The process of fiber formation is affected by the temperature and velocity field of ambient air.

The technology of melt-spinning allows obtaining the fibrous materials a wide range of mechanical and physico-chemical properties, using target-oriented exposure of external

factors, in particular, forced electrization of fibers during their formation.

The use of polarization and electrization techniques in melt-spinning technology is an important technological direction because electret fibrous materials are widely used in modern engineering [5]. The melt-spinning technology can readily be adapted for electret fiber production; simple and low-energy consuming techniques of electret production are known which can combine drawing and electrization in one technological process. Therefore, the effect of technological parameters, electric field intensity, electrode design on the magnitude and stability of the fiber electret charge is of prime interest.

The aim of this paper is to investigate the electret state of melt-spun polypropylene fibers polarized during the formation process and estimate the effect of technological parameters on the magnitude and stability of the fiber electret charge.

2. Experimental method

Polypropylene fibers were produced using the melt-spinning installation. The multi-spinneret head allowed simultaneous drawing of 12–48 filaments. The drawing rates used were 2000 and 3000 m/min; the temperature in the extruder was 245–250 °C.

Forced electrization in static (corona discharge) and alternating electric fields was used to affect the electret

* Corresponding author.

E-mail address: kravtsovag@mail.ru (A.G. Kravtsov).

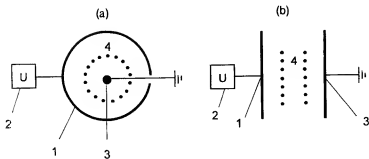


Fig. 1. The system of polarization electrodes (top view): Scheme 1 (a); Scheme 2 (b). 1, high-voltage electrode; 2, voltage source; 3, grounded electrode; 4, fibers under polarization.

state of the fibers. Two different electrode designs were used (Fig. 1).

Electrode (1) was connected to a high-voltage source (2) and the electrode (3) was grounded. The fibers (4) passed between the electrodes (1) and (2). In the experiments, the electrode system was placed at the following distances, h , from the spinning die:

- $h = 50$ cm—the region of melt flow—the fibers have high flowing quality;
- $h = 70$ cm—the region of fiber formation—the fibers are in the viscous flow state;
- $h = 110$ cm—the region of formed fibers—the fibers are in a solid (crystalline) phase and keep their shape.

In several experiments, two high-voltage sources connected in parallel were used to apply the static and alternating electric fields together.

The dielectric parameters of the electret fibers were determined using the Novocontrol Chelsea dielectric interface (impedance) gain-phase analyzer 1260 (Instrument Division, UK).

To characterize the electret state of the fibers, the thermally stimulated depolarization technique was used. The thermally stimulated current (TSC) of fibrous specimens was measured at the heating rate of 5 K/min [6]. The specimen size was $30 \times 30 \times 2$ mm³. The effective surface charge density, σ_{eff} , was measured by the non-contact compensation technique [7]. The melting temperature of the specimens was determined using the differential thermal analysis.

3. Results and discussion

It is well known that TSCs in electrets are the result of several different processes whose general cause is the tendency to recover electrical neutrality [8]. In electrets made of polar substances depolarization is mainly due to disordering of dipoles; in non-polar materials it is due to motion of free charges. Consider what processes determine TSC in melt-spun PP electret fibers.

3.1. Spontaneous polarization

Fig. 2 presents TSC spectra of non-polarized melt-spun polypropylene fibers. The TSC peaks and the presence of the effective surface charge, σ_{eff} , in the specimens, are probably due to spontaneous polarization. The mechanism of spontaneous electret effect in melt-spun fibers can be represented as follows.

First, to afford sufficient melt flow, extrusion of polymer materials during the melt-spinning process is carried out at elevated temperatures, which can result in intensive thermal oxidation. During the polymer heating, elongation of chemical bonds takes place according to the thermal fluctuation mechanism. At sufficiently large elongation (melt overheating), auto-ionization of macromolecules through bond breakage accompanied by electron break-off can occur—a bound electron leaks under the potential barrier due to the tunnel effect [9]. The probability of such auto-ionization in the melt-spinning process is rather high.

Secondly, macromolecules having "inborn" defects, such as specifically oriented atomic groups with large permanent or induced dipole moment are inevitably present in the PP

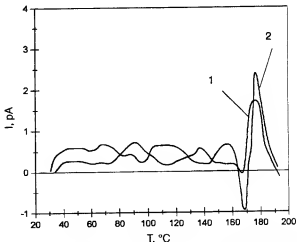


Fig. 2. TSC spectra of non-polarized melt-spun polypropylene fibers. 1, drawing rate $v = 2000$ m/min, effective surface charge density $\sigma_{\text{eff}} = 0.09$ nC/cm²; 2, $v = 3000$ m/min, $\sigma_{\text{eff}} = 0.12$ nC/cm².

melt. These defects can act as structural traps [10]. When PP melt gets in contact with metal parts of the melt-spinning installation, charge carriers injected from the metal are localized at these “trapping centers”.

Thirdly, the charges captured by the fibers at the high-temperature stage of the drawing process are stable enough. Due to fast cooling of the fibers at the following stages, these charges cannot leave their traps and remain “frozen” in the polymer.

Fourth, it can be assumed that triboelectrization contributes much to the spontaneous fiber polarization, which is evidenced by higher TSC peaks and increased surface charge, σ_{eff} , at increased drawing rates.

Thus, it can be concluded that spontaneous polarization of melt-spun fibers is governed by the technology of the melt-spinning process.

It is obvious that if forced fiber polarization is used, the electret state of fibers also should considerably depend on technological parameters.

3.2. The electrode shape

Figs. 3 and 4 show that different design of polarizing electrodes result in different charge state of the fibers. TSC spectra of fibers polarized using Scheme 1 (see Fig. 1a) consist of diffuse peaks, which can overlap one another (Fig. 3). On the contrary, the fibers charged using Scheme 2 (see Fig. 1b) exhibit distinct sharp TSC peaks. Peaks at $T_{\text{max}} = 170\text{--}175\text{ }^{\circ}\text{C}$ illustrate the charge relaxation which is due to PP melting.

It should be noted that the surface charge density is somewhat higher for the fibers charged using Scheme 1.

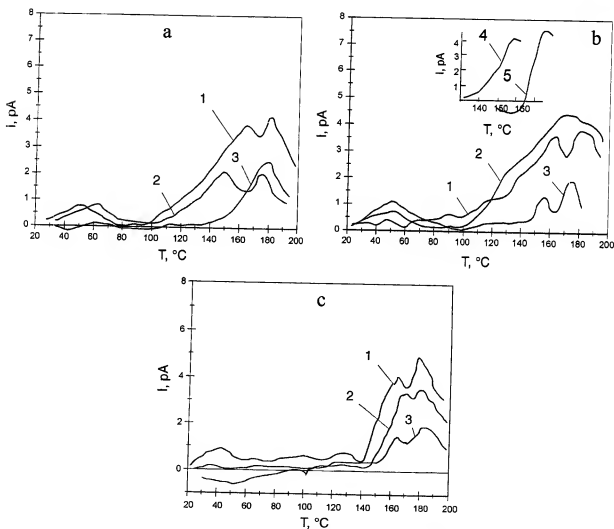


Fig. 3. TSC spectra of melt-spun polypropylene fibers polarized using Scheme 1. (a) $h = 110\text{ cm}$; $v = 2000\text{ m/min}$; effective surface charge densities for curves 1–3; respectively: $\sigma_{\text{eff}1} = 10.3\text{ nC/cm}^2$; $\sigma_{\text{eff}2} = 7.4\text{ nC/cm}^2$; $\sigma_{\text{eff}3} = 6.0\text{ nC/cm}^2$. (b) $h = 70\text{ cm}$; $v = 2000\text{ m/min}$; $\sigma_{\text{eff}1} = 12.2\text{ nC/cm}^2$; $\sigma_{\text{eff}2} = 8.3\text{ nC/cm}^2$; $\sigma_{\text{eff}3} = 7.1\text{ nC/cm}^2$. (c) $h = 70\text{ cm}$; $v = 3000\text{ m/min}$; $\sigma_{\text{eff}1} = 11.0\text{ nC/cm}^2$; $\sigma_{\text{eff}2} = 7.4\text{ nC/cm}^2$; $\sigma_{\text{eff}3} = 7.0\text{ nC/cm}^2$. Polarization conditions: curve 1, in a corona discharge (electric field intensity $E = 10\text{ kV/cm}$); curve 2, under combined action of the corona discharge and the alternating electric field (the amplitude of the alternating electric field intensity $E_{\text{ab}} = 9\text{ kV/cm}$); curve 3, in alternating electric field only; curves 4 and 5, after initial thermal clearing.

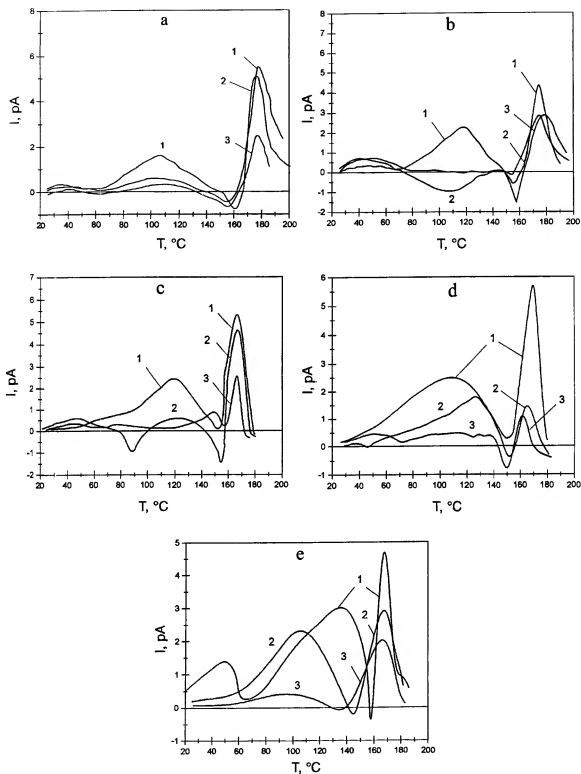


Fig. 4. TSC spectra of melt-spun polypropylene fibers polarized using Scheme 2. (a) $h = 110$ cm; $v = 3000$ m/min; $\sigma_{eff1} = 9.8$ nC/cm²; $\sigma_{eff2} = 6.4$ nC/cm²; $\sigma_{eff3} = 5.7$ nC/cm². (b) $h = 70$ cm; $v = 2000$ m/min; $\sigma_{eff1} = 11.9$ nC/cm²; $\sigma_{eff2} = 7.0$ nC/cm²; $\sigma_{eff3} = 5.4$ nC/cm². (c) $h = 50$ cm; $v = 2000$ m/min; $\sigma_{eff1} = 13.9$ nC/cm²; $\sigma_{eff2} = 10.4$ nC/cm²; $\sigma_{eff3} = 5.9$ nC/cm². (d) $h = 70$ cm; $v = 3000$ m/min; $\sigma_{eff1} = 10.6$ nC/cm²; $\sigma_{eff2} = 7.1$ nC/cm²; $\sigma_{eff3} = 4.0$ nC/cm². (e) $h = 50$ cm; $v = 3000$ m/min; $\sigma_{eff1} = 12.1$ nC/cm²; $\sigma_{eff2} = 8.8$ nC/cm²; $\sigma_{eff3} = 4.8$ nC/cm². Polarization conditions as in Fig. 3.

The differences in electret charge formation with different electron shapes can be explained as follows. It is assumed that the fiber has round cross-section, then in Scheme 1 practically the whole space between the electrodes is the polarization region, and practically the whole fiber surface undergoes polarization. Obviously, for Scheme 2 it is not the case—only a half of the surface (oriented towards the high-voltage electrode) is polarized, which results in less intense electrization and lower values of parameters characterizing the electret effect.

3.3. The distance between the spinning die and the electrodes

The distance, h , between the spinning die and the electrodes is another important parameter which affects the charge state of the fibers.

The analysis of the TSC spectra (Figs. 3 and 4) shows that in all cases the intensity of the peaks increased as the distance h decreased. This dependence is especially prominent for Scheme 2, whereas in the case of Scheme 1 it is less distinct. However, the effective surface charge, σ_{eff} , increased at lower h for all specimens. This can probably be attributed to the fact that in Scheme 1 the electrization is more intensive and mainly “deep”, i.e., trapped charges are distributed mostly in the depth of the fiber. At lower h , hot melt, in which only a part of deep traps has yet been formed, is polarized and charge carriers are trapped both at the surface and in the bulk. This is confirmed by the form of the TSC spectra and high σ_{eff} values for these specimens. At higher h , the fiber temperature decreases, resulting in lower probability of surface trapping; however, the tendency of deep trapping remains.

3.4. Fiber drawing rate

The experiments have shown that the effective surface charge, σ_{eff} , decreased slightly as the drawing rate increased from 200 to 3000 m/min. For Scheme 2, the intensity of TSC peaks increased to some extent in the case of corona discharge, and decreased when alternating electric field was applied. For Scheme 1, no distinct effect of drawing rate on the electret charge was revealed.

Obviously, this result can be attributed to the effect of several simultaneous concurring processes, such as fiber polarization in the electric field, thinning of fibers under drawing and fiber cooling. When Scheme 1 is used, the limiting factor is the exposure time. For the conditions characteristic of Scheme 2, the fiber temperature seems to be more important: even short-time polarization of hotter fibers results in stronger electret effect.

3.5. Electret charge formation under action of static and alternating electric field

Injection of charge carriers into a polymer was considered by several researchers [11–13], who analyzed in detail

chemical processes accompanying injection. The interaction of charged particles with the polymer (in this work, polypropylene) results in the polarization of the latter.

In the gap between the electrode and the polymer surface, the flow of charged particles induces ionization of air molecules, including electron detachment and breaking of covalent bonds in gas molecules. As a result, positive and negative ions and free electrons appear in the gap [14]. Chain chemical reactions take place in this region; at high electric field intensity (or high energy of charge carriers), these are accompanied by visible or ultraviolet radiation.

In the case of corona discharge, positively charged particles move to the cathode where they are neutralized and negatively charged ones move to the fiber surface. Ions are trapped at the depth of several molecular layers under the surface and electrons penetrate into the bulk of the polymer [12]. These charged particles can cause, in an electric field and under elevated temperature, several physicochemical phenomena:

1. Trapping of charge carriers by various structural defects of the polymer, impurities, voids, end groups.
2. Trapping of charge carriers at interfaces melt/crystalline phase/amorphous phase.
3. “Self-trapping” of electrons in the polymer bulk, when a high-energy electron produces a structural defect and gets trapped in it.
4. Thermal destruction of the polymer, resulting in formation of polar groups and charged fragments of molecules.
5. Formation of ozone, atomic oxygen and nitrogen oxides in the air gap under the action of an electric field, following by macromolecules oxidation and polar group formation.
6. Heterolytic breakage of chemical bonds in polymers, when a macromolecule falls apart into charged fragments. These fragments possess dipole moment and can be responsible for dipole polarization. The formed dipoles are oriented in the electric field of the corona discharge and then are “frozen” upon melt solidification.

Thus, in an electric field of sufficient intensity, existing around a corona discharge, many processes can lead to the formation of an electret which shows both dipole and “injection” polarization. Due to the complex character of the phenomenon, it is rather difficult to reliably determine parameters of trapping levels and differentiate between hole and electron traps.

As can be seen in the TSC spectra (Figs. 3 and 4, curve 1), three TSC peaks are characteristic of polypropylene fibers treated by a corona discharge. The first peak ($T_{\text{max}} = 50\text{--}60\text{ }^{\circ}\text{C}$) is attributed, in all probability, to Maxwell-Wagner polarization [15], i.e., electric charge is localized at interfacial trapping sites due to the difference in electrical conductivity of the phases. The intensity of this peak is rather low. The second (medium-temperature) peak ($T_{\text{max}} = 150\text{--}165\text{ }^{\circ}\text{C}$, Fig. 3; $110\text{--}120\text{ }^{\circ}\text{C}$, Fig. 4) can be due to the

release of both inherent and injected charge carriers as well as disorientation of the dipole groups. The third peak (170–175 °C) reflects the release of injected charges and corresponds to the melting temperature.

In all probability, Scheme 1 increases the contribution of injected charges to the total electret effect but decreases, to some extent, dipole polarization. In the gap between the electrodes in Scheme 1, the probability of a certain dipole orientation is statistically lower and the probability of injection is greater.

In an alternating electric field, the general appearance of the TSC spectra is similar; however, the peaks are much less intense. For instance, the medium-temperature peak in Figs. 3 and 4 (curve 3) is very low. Probably the formation of oriented dipoles is more characteristic of the corona discharge. In an alternating field, the polymer oxidation accompanied by polar group formation also takes place, but the probability of dipole orientation is considerably less. All other above-mentioned factors act in an alternating field with lesser intensity, which may be attributed to different energy of charge carriers.

The wider TSC peaks characteristic of Scheme 1 are probably due to structural traps of different origin—and consequently having different parameters—are filled. Under heating during the TSC measurement, charge carriers are released “stepwise”. Sometimes the peaks may overlap, resulting in one wider peak (see Fig. 3b, curve 2). Using the “initial temperature clearing” technique [15], it was possible to separate such peaks (Fig. 3b, curves 4 and 5).

For the samples obtained under simultaneous action of the alternating field and the corona discharge, the TSC peak intensity was less than that treated in the corona discharge only (see Figs. 3 and 4, curve 2). In all probability, it is the effect of the field anisotropy which causes dipole disorientation and lowers the charge carrier energy.

4. Conclusion

The melt-spinning technology favors formation of spontaneous electret charge in melt-spun fibers; the magnitude of this charge is a function of technological parameters. Forced fiber polarization in external electric fields gives rise to strong electret effect. Different mechanisms, such as Maxwell–Wagner polarization, dipole orientation, charge

carrier injection, contribute to the total electret effect in the fibers.

The electret state of melt-spun fibers can be controlled by changing the parameters of the process of fiber formation. For instance, the electret charge can be affected by using polarizing electrodes of different shape. Fiber polarization according to Scheme 1 results in wide, sometimes overlapping TSC peaks and higher surface charge density as compared with Scheme 2. At higher drawing rates, the electret charge decreases slightly, which may be as result of the shorter time the fiber is exposed to the polarizing field. Fiber polarization in the hot state is more effective than their polarization in the solid crystalline phase.

The effect of static and alternating electric fields on the electret state of melt-spun fibers has been studied. The mechanism of electric field action is rather complicated and requires further thorough investigation. The corona discharge was found to be more effective for fiber polarization than its combination with an alternating field and the alternating field only.

References

- [1] R. Beyreuther, R. Barthel, W. Nicht, *Acta Polym.* 30 (5) (1970) 308–312.
- [2] R. Beyreuther, R. Barthel, W. Nicht, *Acta Polym.* 30 (9) (1970) 592–596.
- [3] R. Beyreuther, H. Brüning, R. Vogel, in: J.C. Salamone (Ed.), *Polymeric Materials Encyclopedia*, Vol. 6, CRC Press, New York, 1986, pp. 4061–4074.
- [4] H. Brüning, *Chem. Fibers* 4 (1994) 35–40.
- [5] L.S. Pincuk, V.A. Goldade, *Electret Materials in Engineering*, Infotribo, Gomel, 1998 (in Russian).
- [6] Yu.A. Gorohvatsky, H.A. Bordovsky, *Thermally Stimulated Current Spectroscopy of High-resistance Semiconductors and Dielectrics*, Nauka, Moscow, 1998.
- [7] A.I. Gubkin, *Electrets*, Nauka, Moscow, 1991.
- [8] I.B. Lushcheykin, *Polymer Electrets*, Nauka, Moscow, 1984.
- [9] A.I. Gubanov, *Polym. Mech.* 5 (1978) 771.
- [10] L.S. Pincuk, A.G. Kravtsov, Ya.I. Voronzhnev, Yu. Gromyko, *Intern. Polym. Process.* 13 (3) (1998) 67–70.
- [11] C.E. Jowett, *Electrostatics in the Electronics Environment*, Macmillan, New York, 1976, p. 135.
- [12] B.A. Gresswell et al., *Telesis* 2 (1) (1971) 21–26.
- [13] M. Shanon, *J. Chem. Phys.* 45 2600–2605.
- [14] S.D. Chatterjee et al., *J. Franklin Inst.* 289 (1970) 473.
- [15] K.H. Nicholas, J. Woods, *Brit. J. Appl. Phys.* 15 (1964) 783–795.